J. Fluid Mech. (1990), *vol.* 220, *pp.* 355–368
Printed in Great Britain

Shear-layer pressure fluctuations and superdirective acoustic sources

By D. G. CRIGHTON[1] AND P. HUERRE[2]

[1] Department of Applied Mathematics and Theoretical Physics, University of Cambridge, Cambridge CB3 9EW, UK

[2] Département de Mécanique, Ecole Polytechnique, 91128 Palaiseau, France

(Received 6 May 1986 and in revised form 12 June 1990)

We consider a sequence of boundary-value problems for the acoustic wave equation, with the pressure specified on the boundary as a function of space and time, and simulating features of the pressure field measured just outside a turbulent shear layer supporting large-scale coherent structures. The boundary pressure field has the form of a travelling subsonic plane wave, modulated by a large-scale envelope function. Three models for the envelope distribution are studied in detail, and the particular features which they exhibit are shown to be representative of large classes of amplitude functions.

We start by looking at the hydrodynamic near field of the boundary pressure fluctuations, over spatial regions throughout which the motion can be taken as incompressible. Very close to the boundary, the pressure fluctuations decay exponentially with transverse distance, while at sufficiently large distances from the whole wave packet on the boundary, the pressure fluctuations have a dipole algebraic decay. We investigate the transition from exponential to algebraic decay, and find that it is effected through quite a complicated multilayer structure which depends crucially on the detailed form of the envelope.

Acoustic fields are then determined both from exact solutions to the wave equation, and from matching arguments. In some cases, where the boundary source is compact, the distant acoustic fields have a simple compressible dipole type of behaviour. In other cases, however, when the boundary source is non-compact, the acoustic field has a *superdirective* character, the angular variation being described by exponentials of cosines of the angle with the streamwise direction. It is shown how the superdirective acoustic sources are completely compatible with the features of the inner incompressible field, and a criterion for the occurrence of the superdirective acoustic fields will be given. Superdirective fields of this kind have been observed in measurements by Laufer & Yen (1983) on a low-speed round jet of Mach number 0.1, and the general relation of our results to those experiments is explained.

1. Introduction

Laufer & Yen (1983) report experimental studies of the near- and far-field pressure fluctuations associated with a highly ordered vortex-wave structure in a round jet. The jet has very low Mach number (around 0.1), and diameter Reynolds number around 5×10^4. It emerges with a laminar exit boundary layer, and weak acoustic forcing, tuned to the frequency f_0 of maximal spatial instability of the initial shear layer, is used to phase-lock and organize the development of axisymmetric modes on the shear layer and jet column. Under the forcing, the shear layer rolls up into a rather tightly wound ring vortex at a well-defined axial location I; a pair of consecutive vortices so formed travels downstream and merges (the following vortex causing the preceding one to expand and decelerate, allowing the following one to move inside and capture it) at axial location II; and one or two further vortex pairings take place further downstream at III, IV, etc. The spectrum of near-field pressure fluctuations around location I shows a pronounced spike at frequency f_0, with smaller spikes at the subharmonic frequencies $f_1 = \frac{1}{2}f_0$, $f_2 = \frac{1}{4}f_0$, etc., much smaller spikes at the integral harmonics $2f_0$, $3f_0$, etc. and with still weaker spikes at the combination frequencies $(2f_0+\frac{1}{2}f_0)$, $(3f_0-\frac{1}{4}f_0)$, etc. The spikes are connected by a broadband spectrum of low energy. In the absence of forcing the spectrum is broadband and at a much higher level; forcing, even of very low amplitude, phase-locks the fluctuations into the fundamental and subharmonics which are the dominant features of the near-field spectrum.

As one goes downstream from I, the spectral level at f_0 decreases, that at f_1 and f_2 increases, and by II the spectrum is dominated by a tone at f_1, and at III by a tone at f_2, etc. One may therefore think of the processes occurring either as suggested synoptically, in terms of the repeated mergings of ring vortices in a rather sudden, though well-defined, way, or, as suggested by the evolution of the near-field pressure spectrum with axial distance, in terms of a wave model in which modes with frequencies $f_0, f_1, f_2 \ldots$ grow and decay with axial distance. We favour the latter, as more conducive to analysis, especially when it comes to calculating the sound field generated by the waves, and when it comes to understanding the controlling processes. One thing should, however, be stressed. While the ring vortices clearly do interact in a strong way, we do not regard the interactions between the wave components as significant. When viewed from the wave-theory angle, we assert that it is appropriate to regard each of the modes with frequencies $f_0, f_1, f_2 \ldots$ as an independent linear instability of the shear layer. Certainly there is some interaction between the wave modes, but if this interaction were strong, it would also generate much more intense components at the second and third integral harmonic frequencies $2f_0, 3f_0, \ldots$, than are seen. The processes that take place as one proceeds downstream may give the appearance, from the spectral shapes, of merely transferring energy from the fundamental f_0-mode to the first subharmonic, then to the second, and so on. But there is no conservation of energy here, and no reason to correlate the growth of the f_1-mode with the decay of the f_0-mode; each is to be regarded as an independent instability mode, growing because of the basic shear-flow instability, decaying because of the change in the instability characteristics with downstream distance. This near-linear growth and decay is seen explicitly in figure 23 of Laufer & Yen (1983), where the response at a fixed frequency is shown as a function of axial distance and forcing level.

Laufer & Yen (1983) found that this growth and decay of wave amplitude could be described by the relation

$$\langle p^2(x,f_n)\rangle \sim \exp\left[-2\frac{(x-\bar{x}_n)^2}{\lambda_n^2}\right], \tag{1.1}$$

where λ_n is the wavelength of the mode of frequency $f_n (n = 0, 1, 2$ were measured), and $\bar{x}_n$ the location at which the peak amplitude of that mode is attained. Phase measurements were used to infer the wavelengths λ_n. The near-field pressures thus have a wave-packet form at each frequency, with a Gaussian envelope of width $2\lambda_n$. There is, of course, not enough information from which to decide whether the Gaussian is really a decisively better representation than, say, one of the form

$[1+(x^2/\lambda_n^2)]^{-N}$ for some N – but the consequences for the acoustic field of modelling the wave packet with a Gaussian, rather than algebraic, envelope are very striking and will receive much further comment.

Turning now to the acoustic field, one sees in the spectra measured by Laufer & Yen (1983) spikes at all the frequencies detected in the near field, and, in particular, at f_0, f_1 and f_2. The sound fields at these frequencies have a most unusual directivity pattern; it is found for each of them that, if M_c is the phase Mach number of the mode concerned (about 0.5 times the jet exit Mach number for each of f_0, f_1, f_2), then

$$\langle p^2(\theta, f_n)\rangle \sim \exp[90M_c \cos\theta], \tag{1.2}$$

where θ is measured from the downstream direction. We shall refer to acoustic fields of this kind as *superdirective*. For the conditions ($M_c \sim 0.1$) of these experiments, the directivity is essentially of exponential type, and cannot be expanded in a multipole series (in which $\langle p^2\rangle$ would involve terms of *even* degree in $\cos\theta$). One might, of course, expect a directivity characterized by an 'antenna factor' such as appears in (1.2); after all, the wave-packet structure along the jet axis, with a Gaussian envelope, might well be expected to lead to the form (1.2), as indeed it does. But the surprising thing is that the superdirective field (1.2) is generated by a source which is apparently extremely small in comparison with the acoustic wavelength. For the axial length of the packet envelope (1.1) is essentially $2\lambda_n$ at frequency f_n, and the convection Mach number is 0.5×10^{-1} for a jet Mach number of 0.1. Therefore the whole envelope is about 0.1 of an acoustic wavelength in axial extent, while the transverse extent to which significant velocity fluctuations are confined is smaller still, comparable with the shear-layer thickness. Regardless, then, of whether it is possible to predict theoretically the near-field structure observed by Laufer & Yen, one must ask the question, 'How can such a small source generate a superdirective acoustic field?', and the answer to that question is addressed in the present work.

Parenthetically we refer to earlier work (Huerre & Crighton 1983) in which an attempt was indeed made to predict the near- and far-field structure of Laufer & Yen, as represented by (1.1) and (1.2). There we used linear spatial instability theory for a linearly diverging shear layer to predict a wave-amplitude variation with x of precisely the form (1.1), namely a Gaussian envelope whose width at any frequency f is a fixed multiple of the wavelength at that frequency, and, using a standard estimate for the shear-layer growth rate, we obtained (1.1) with the 2 there replaced by 2.2. From these calculations it was possible to determine the radiated acoustic field from a straightforward application of Lighthill's (1952) aeroacoustic theory, retarded-time differences along the jet axis being retained in the calculation, even though the axial extent of the source region appeared to be small compared with the wavelength of sound. Despite an apparently reasonable prediction of the near-field structure, we were unable to reproduce (1.2). Our result for $\langle p^2\rangle$ contained an antenna factor of the right form, but with an underestimate of the exponent, $\exp[52M_c\cos\theta]$, while we had also other terms which caused large variations of directivity which were not seen in the measurements. We shall return to this issue in a future paper with P. A. Monkewitz; here we are concerned only to understand how an apparently 'small' source of suitable structure can generate a superdirective acoustic field – though as part of this we shall make some specific predictions about the decay of near-field pressure fluctuations which are in themselves interesting and should be capable of experimental study.

In §2 we study the decay of those near-field fluctuations in the context of a set of model problems in which the pressure $p(x, y, t)$ in a two-dimensional unsteady flow is *specified* on the boundary in wave-packet form,

$$p(x, 0, t) = A(\epsilon x) \exp(\mathrm{i}x - \mathrm{i}t), \tag{1.3}$$

$\exp(\mathrm{i}x - \mathrm{i}t)$ referring to the fast-scale oscillations, $A(\epsilon x)$ to slow amplitude modulation, with $\epsilon \ll 1$. Equation (1.3) mimics the near-field structure of the Laufer–Yen experiments. In $y > 0$ the flow is irrotational and of small amplitude (there is no mean flow there) and Laplace's equation

$$\frac{\partial^2 p}{\partial x^2} + \frac{\partial^2 p}{\partial y^2} = 0 \tag{1.4}$$

governs the decay of the pressure field with y. Incompressible fluctuations are assumed in §2, and the effects of compressibility included in §3. Ignoring the time factor $\exp(-\mathrm{i}t)$ throughout, it is clear that sufficiently close to the boundary $y = 0$, the decay with y is exponential,

$$p(x, y) \sim A(0) \exp(\mathrm{i}x - y), \tag{1.5}$$

and indeed such exponential decay has been seen on many occasions in experimental study of wave-like motions in shear layers (see, for example, Gutmark & Ho 1985; Lafouasse, Chan & Ho 1986). Ultimately, however, as $r \to \infty$ ($x = r\cos\theta$, $y = r\sin\theta$, $0 < \theta < \pi$) the field is that of a concentrated dipole whose strength F_0 is the instantaneous force applied to the boundary,

$$p(r, \theta) \sim \frac{1}{\pi} F_0 \frac{\sin\theta}{r}, \tag{1.6}$$

with

$$F_0 = \int_{-\infty}^{+\infty} A(\epsilon x)\, \mathrm{e}^{\mathrm{i}x}\, \mathrm{d}x. \tag{1.7}$$

We are interested in the manner in which the decay changes from exponential to algebraic around some penetration distance – and more generally we are interested in the structure of solutions to (1.3) and (1.4), for $\epsilon \ll 1$, throughout $-\infty < x < +\infty$, $0 < y < +\infty$. It is easy to write down, in several different forms, a general integral solution to the problem, and to verify the laws (1.5) and (1.6) in general. But there is no universal way in which the exponential–algebraic transition is achieved, and indeed much of the emphasis here is to show that there are a variety of completely different routes, for each of which there are different features in the acoustic field of §3. We therefore start with examples, choosing specific forms $A(\epsilon x)$ for which the complete asymptotic structure of $p(x, y, \epsilon)$ in the (x, y)-plane can be displayed. Two of our three examples are, naturally, the Gaussian $\exp(-\epsilon^2 x^2)$ and the algebraic $(1 + \epsilon^2 x^2)^{-1}$ for $A(\epsilon x)$; the third is $\exp(-\epsilon|x|)$ which, although artificial near $x = 0$, gives a third asymptotic structure quite different from the other two.

We then give a general argument for determining the 'penetration distance' in terms of properties of $A(\epsilon x)$ (although no detailed description of the structure in the (x, y)-plane seems possible), and will show that envelope functions whose Fourier transforms have higher-order Gaussian decay, $\hat{A}(K) \sim \exp(-|K|^{2n})$, with $n \geqslant 2$, yield arbitrarily large penetration distances for a fixed physical envelope width $|x| \lesssim \epsilon^{-1}$. We should also stress that the exponential decay of (1.5) does not persist in this simple form all the way to the penetration distance, and that distance should really be thought of as (*a*) the distance beyond which the ultimate dipole decay applies, and (*b*) the distance beyond which the memory in $p(x,y)$ of the phase structure $\exp(\mathrm{i}x-\mathrm{i}t)$ imposed at $y=0$ is completely eradicated.

These features are essential to an understanding of the acoustic field, in a way which will be explained in §3. In §3 we shall also show that the features of the acoustic field are actually fully consistent with standard acoustic theory. The reason is that the source scale relevant to the acoustic field is not the envelope width, but the integral scale $\int_{-\infty}^{+\infty} A(\epsilon x)\exp \mathrm{i}x\,\mathrm{d}x$. For a Gaussian envelope the integral scale is $O(\epsilon^{-2})$, much larger than the envelope scale because of the substantial phase cancellation that takes place over the envelope region $|x| < O(\epsilon^{-1})$ in which A is effectively constant. Superdirective behaviour is seen in §3 to take place when the integral scale is comparable with the acoustic wavelength – the standard condition – even though the apparent source size is vanishingly small on the wavelength scale. An alternative requirement for superdirective behaviour is deduced in §3 from matching arguments, and states that the penetration distance should be comparable with the wavelength; and since it is shown in §3 that the penetration distance and integral scale are comparable, this alternative is entirely equivalent to the standard condition of comparability of integral scale and wavelength.

Section 4 deals briefly with application to the experiments of Laufer & Yen (1983). A more complete explanation of those experiments, including the calculation of $A(\epsilon x)$ from linear and nonlinear instability theory, will be published elsewhere.

2. Decay of incompressible pressure fluctuations

The problem to be studied is, as explained in §1, defined by

$$\left.\begin{aligned} p_{xx}+p_{yy} &= 0 \quad (-\infty < x < +\infty, y > 0),\\ p(x,0) &= A(X)\exp(\mathrm{i}x), \end{aligned}\right\} \tag{2.1}$$

where we write $(X, Y) = (\epsilon x, \epsilon y)$ and suppress a factor $\exp(-\mathrm{i}t)$. The general solution can be written

$$p(x,y) = \int_{-\infty}^{+\infty} F(k)\exp(\mathrm{i}kx-|k|\,y)\,\mathrm{d}k, \tag{2.2}$$

where

$$\begin{aligned} F(k) &= \frac{1}{2\pi}\int_{-\infty}^{+\infty} A(\epsilon x)\,\mathrm{e}^{-\mathrm{i}(k-1)x}\,\mathrm{d}x \\ &= \frac{1}{\epsilon}\hat{A}\left(K = \frac{k-1}{\epsilon}\right), \end{aligned} \tag{2.3}$$

and

$$\hat{A}(K) = \frac{1}{2\pi}\int_{-\infty}^{+\infty} A(X)\exp(-\mathrm{i}KX)\,\mathrm{d}X \tag{2.4}$$

defines the Fourier transform $\hat{A}(K)$ of $A(X)$. Thus

$$p(x,y) = \frac{1}{\epsilon}\int_{-\infty}^{+\infty} \hat{A}\left(\frac{k-1}{\epsilon}\right)\exp(\mathrm{i}kx-|k|\,y)\,\mathrm{d}k, \tag{2.5}$$

or

$$p(X,Y) = \int_{-\infty}^{+\infty} \hat{A}\left(K-\frac{1}{\epsilon}\right)\exp(\mathrm{i}KX-|K|\,Y)\,\mathrm{d}K, \tag{2.6}$$

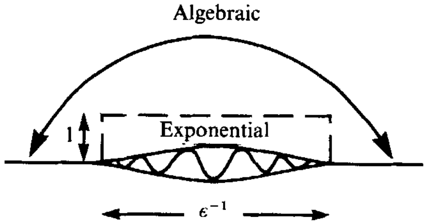

FIGURE 1. Case A: exponential $A(X)$.

and we now choose three forms for $A(X)$ which allow these integrals to be expressed in terms of known functions, and their asymptotic structure as $\epsilon \to 0$ to be ascertained for all (x, y).

Case A. Exponential $A(X) = \exp(-|X|)$,

$$\hat{A}(K) = [\pi(1+K^2)]^{-1}. \tag{2.7}$$

One finds, for $x > 0$,

$$p = \exp\{\mathrm{i}x - y - (X + \mathrm{i}Y)\} - \frac{\mathrm{i}}{2\pi}\exp\left[\left(\frac{\mathrm{i}}{\epsilon} - 1\right)(X - \mathrm{i}Y)\right]\mathrm{Ei}\left[-\left(\frac{\mathrm{i}}{\epsilon} - 1\right)(X - \mathrm{i}Y)\right], \tag{2.8}$$

plus three similar products of exponential and exponential–integral functions. Detailed analysis shows the following: if $X = O(1)$ and $y = O(1)$, the first term, p_1, in (2.8), is in order of magnitude,

$$p_1 \sim \mathrm{e}^{-y-X} = O(1),$$

while the sum, p_2, of the four terms involving Ei-functions, is $O(\epsilon^2)$. However, when $y > O(1)$, p_1 is exponentially small, $p_1 = O(\mathrm{e}^{-1/\epsilon})$ when $Y = O(1)$, and then $p_2 = O(\epsilon^2)$ dominates. Exponential decay in y thus persists only throughout the rectangular domain $x \leqslant O(\epsilon^{-1})$, $y \leqslant O(1)$ and is immediately followed outside this domain by the ultimate decay

$$p \sim p_2 \sim \frac{2Y\epsilon^2}{(X^2 + Y^2)}, \tag{2.9}$$

which comes from the asymptotic expansion of the Ei-functions and is in agreement with the general form (1.6). Here, then, exponential decay gives way to algebraic at distances a little greater than one wavelength/2π away from the boundary, details of the transition being supplied by the Ei-functions. The situation is illustrated schematically in figure 1.

Case B. Algebraic $A(X) = (1 + X^2)^{-1}$,

$$\hat{A}(K) = \tfrac{1}{2}\exp(-|K|). \tag{2.10}$$

One finds simply

$$p = \frac{1}{2}\frac{\exp\left\{-\dfrac{1}{\epsilon}(Y - \mathrm{i}X)\right\}}{(Y + 1 - \mathrm{i}X)} + \tfrac{1}{2}\mathrm{e}^{-1/\epsilon}\frac{\left[1 - \exp\left\{-\dfrac{1}{\epsilon}(Y - 1 - \mathrm{i}X)\right\}\right]}{(Y - 1 - \mathrm{i}X)} + \tfrac{1}{2}\mathrm{e}^{-1/\epsilon}\frac{1}{(Y + 1 + \mathrm{i}X)}, \tag{2.11}$$

but the structure represented by this is quite complicated, and indicated roughly in figure 2. Exponential decay persists in this case out to $y = O(\epsilon^{-1})$, and 'above' this

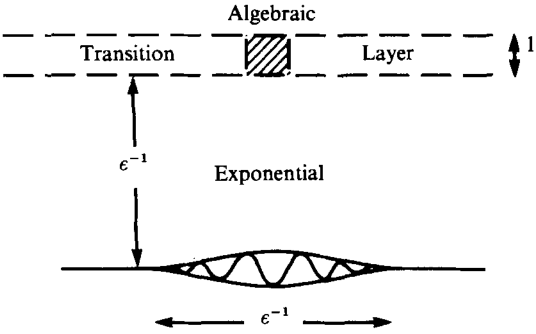

FIGURE 2. Case B: algebraic $A(X)$.

level (in fact for $Y > 1+O(\epsilon)$) there is algebraic variation – though the algebraic variation itself is not of the ultimate form (1.6) until $X^2+Y^2 \gg 1$. The transition from exponential to algebraic is effected by a boundary layer and a central zone, as indicated in figure 2. The central zone is of width $O(1)$ in the fast (x, y) variables, and is centred on $Y = 1$, $X = 0$. It is surrounded by a layer $|Y-1| = O(\epsilon)$, transition through the central zone being described by different expressions from those that govern transition through the surrounding layer.

The essential contrast with Case A is that, whereas there the penetration depth for exponential decay was $y \sim O(1)$, here it is much larger, $y \sim O(\epsilon^{-1})$, comparable with the envelope scale rather than with the wavelength.

Observe also that, whereas in the algebraic decay region for Case A one has $p = O(\epsilon^2)$ for fixed (X, Y), here in Case B one has, again for fixed (X, Y), $p = O(\mathrm{e}^{-1/\epsilon})$.

Case C. Gaussian $A(X) = \exp(-X^2)$,

$$\hat{A}(K) = \frac{1}{2\pi^{\frac{1}{2}}}\exp(-\tfrac{1}{4}K^2). \tag{2.12}$$

Here one finds

$$\begin{aligned} p(x,y) &= \tfrac{1}{2}\exp(\mathrm{i}z-\epsilon^2z^2)\,\mathrm{erfc}\left\{-\epsilon\left(\mathrm{i}z+\frac{1}{2\epsilon^2}\right)\right\} \\ &\quad +\tfrac{1}{2}\exp(\mathrm{i}z^*-\epsilon^2z^{*2})\,\mathrm{erfc}\left\{+\epsilon\left(\mathrm{i}z^*+\frac{1}{2\epsilon^2}\right)\right\} \\ &= p_1+p_2, \end{aligned} \tag{2.13}$$

say, with $z = x+\mathrm{i}y$, $z^* = x-\mathrm{i}y$. For $x^2+y^2 \ll \epsilon^{-2}$,

$$p_1 = \mathrm{e}^{\mathrm{i}z-\epsilon^2z^2}+O(\epsilon\,\mathrm{e}^{-1/4\epsilon^2}), \tag{2.14}$$

while

$$p_2 = \frac{\epsilon\,\mathrm{e}^{-1/4\epsilon^2}}{\pi^{\frac{1}{2}}(1+2\mathrm{i}\epsilon^2z^*)}\{1+O(\epsilon)\}, \tag{2.15}$$

where the error is uniform for all x and all $y \geqslant 0$. There is, therefore, certainly exponential decay throughout $x^2+y^2 \ll \epsilon^{-2}$, and in fact the estimate (2.14) for p_1 holds unless

$$|1-2\epsilon^2y| \leqslant O(\epsilon) \quad \text{and} \quad |\epsilon^2x| \leqslant O(\epsilon),$$

as can be seen by writing

$$y = \frac{1}{2\epsilon^2}+\frac{1}{\epsilon}\tilde{Y}, \quad x = \frac{1}{\epsilon}\tilde{X}, \tag{2.16}$$

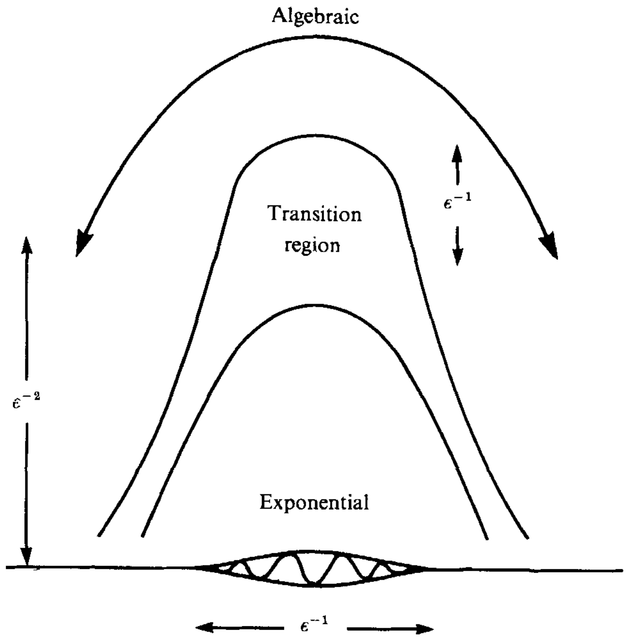

FIGURE 3. Case C: Gaussian $A(X)$.

when one has, exactly,

$$p_1 = \tfrac{1}{2}\mathrm{e}^{-1/4\epsilon^2}\exp\{-(\tilde{X}+\mathrm{i}\tilde{Y})^2\}\,\mathrm{erfc}\{-\mathrm{i}(\tilde{X}+\mathrm{i}\tilde{Y})\}. \tag{2.17}$$

From (2.15) and (2.17) one sees that exponential decay persists for $(x, y) \ll \epsilon^{-2}$, with a transition around $y = 1/2\epsilon^2$ described entirely by p_1.

In the experiments of Lafouasse *et al.* (1986), near-field pressure contours were measured for the first and second subharmonics (f_1 and f_2), in conditions essentially identical to those in Laufer & Yen (1983). The appropriate value of ϵ is then $(2\pi)^{-1}$ (see §4), and one finds then that the shapes of the contours measured by Lafouasse *et al.* (1986) are quite well predicted by those of the dominant term in (2.14), namely hyperbolic curves $\epsilon^2(x^2-y^2)-y =$ constant, with appropriate origins of (x, y).

Equation (2.17) has exponential or algebraic behaviour depending upon the phase of $\tilde{X}+\mathrm{i}\tilde{Y}$, as well as its magnitude, and the shape of the transition region is essentially as depicted in figure 3. The transition-region shape is found by writing down uniform asymptotics to (2.17) for large $(\tilde{X}, \tilde{Y})$, and the transition takes place where

$$2-\frac{1}{\pi^{\frac{1}{2}}}\frac{\mathrm{e}^{\tilde{Z}^2}}{\mathrm{i}\tilde{Z}} \approx 0. \tag{2.18}$$

If ζ is a coordinate normal to the lines

$$\tilde{Z} = \tilde{R}\,\mathrm{e}^{-\pi\mathrm{i}/4} \quad \text{and} \quad \tilde{Z} = \tilde{R}\,\mathrm{e}^{-3\pi\mathrm{i}/4},$$

this requires

$$\tilde{R}^{-1}\exp(\tilde{R}\zeta) = O(1), \tag{2.19}$$

and thus $\zeta = O(\tilde{R}^{-1}\ln\tilde{R})$. Beyond the transition region, p_1 and p_2 are comparable, and combine to give

$$p \sim \frac{1}{\pi^{\frac{1}{2}}}\mathrm{e}^{-1/4\epsilon^2}\left(\frac{\sin\theta}{R}\right), \tag{2.20}$$

which is in accord with (1.6), and has the gauge function $\exp(-\frac{1}{4}\epsilon^2)$, to be contrasted with $e^{-1/\epsilon}$ for Case B and ϵ^2 for Case A.

Again we see a completely different route from exponential to algebraic decay from that of Cases A and B. Perhaps the most striking feature of Case C is that *the exponential decay, and the phase structure in x which that decay carries with it, persists to distances $y \sim \epsilon^{-2}$ from the boundary* – distances not only large compared with the wavelength, but large compared with the envelope scale. This is the key to generation of a superdirective field when compressibility is included, as will be shown in the next section.

Having seen the detailed structure in three special cases, we now look at the general criterion that determines the penetration distance. The dipole expression (1.6) is, of course, no more than the first term in the expansion of (2.6) for large R. Taking a further term, we have

$$p \sim \int_{-\infty}^{+\infty} \left[\hat{A}\left(-\frac{1}{\epsilon}\right) + K\frac{\partial \hat{A}}{\partial K}\left(-\frac{1}{\epsilon}\right)\right] e^{iKX-|K|Y}\,dK$$

$$= \hat{A}\left(-\frac{1}{\epsilon}\right)\frac{2\sin\theta}{R} - i\frac{\partial \hat{A}}{\partial K}\left(-\frac{1}{\epsilon}\right)\frac{4\sin\theta\cos\theta}{R^2}, \tag{2.21}$$

and the penetration distance Δ can be estimated as the value of R at which the expansion (2.21) becomes disordered. This gives

$$\Delta \sim \left[\frac{\partial}{\partial K}\ln \hat{A}(K)\right]_{K=-\frac{1}{\epsilon}}, \tag{2.22}$$

from which the estimates

$$\Delta \sim \epsilon, 1, \epsilon^{-1}$$

for Cases A, B, C, respectively, are immediately recovered. It also follows immediately that

$$\Delta \sim \epsilon$$

whenever $\hat{A}(K)$ vanishes algebraically as $|K| \to \infty$, and that $\Delta \sim 1$ whenever $\hat{A}(K)$ vanishes exponentially (i.e. $\hat{A}(K) \sim |K|^m \exp(-\alpha|K|)$ as $|K| \to \infty$ for some $\alpha > 0$ and $m \gtrless 0$). If, however, $\hat{A}(K)$ has higher-order Gaussian behaviour as $|K| \to \infty$,

$$\hat{A}(K) \sim |K|^m \exp(-\alpha |K|^{2n}),$$

say, then

$$\Delta \sim \epsilon^{-(2n-1)}, \tag{2.23}$$

and *the penetration depth becomes arbitrarily large for a fixed wave envelope width* (unity in the X-variable). The properties of the envelope function $A(X)$ corresponding to these higher-order Gaussian transforms are not well documented, but their behaviour as $|X| \to \infty$ is easily ascertained. Taking

$$\hat{A}(K) = \exp(-|K|^{2n})$$

for definiteness, we have

$$A(X) = x^{1/(2n-1)} \int_{-\infty}^{+\infty} \exp\{-X^{\frac{2n}{2n-1}}(u^{2n} + iu)\}\,du \tag{2.24}$$

for $X > 0$, and a similar expression for $X < 0$. The saddle-point method can be used, and it is evident that this will lead to a decay like $\exp\{-X^{\frac{2n}{2n-1}}\}$, more rapid than simple exponential, less rapid (for $n \geqslant 2$) than Gaussian, and that the decay will in general be oscillatory rather than monotonic.

We have thus seen how the three cases in which the asymptotic structure over the whole (x, y)-plane can be delineated do in fact characterize much larger classes of behaviour, and we have given a general condition by which the penetration distance Δ (in (X, Y) variables) can be determined simply in terms of the behaviour of $\hat{A}(K)$ for large K.

Now it is natural to think of calculating aerodynamic sound emission from low-speed flows by matched expansions, with the Mach number as the small parameter. This will be discussed in the next section. However, as a precursor one might consider trying to derive the results presented above for the three special cases, using perturbation methods for $\epsilon \ll 1$ that do not rely on knowledge of the exact solution. This proves to be surprisingly difficult, and we cannot give a convincing demonstration because there is on the one hand a variety of unexpected asymptotic structures and on the other the difficulty of dealing simultaneously with boundary-layer approximations and multiple-scale expressions.

3. Compressible fields

If the pressure fluctuations take place in static compressible fluid, the problem replacing (2.1) is

$$\left.\begin{aligned} &\frac{\partial^2 p}{\partial x^2}+\frac{\partial^2 p}{\partial y^2}+M_c^2 p = 0, \\ &p(x,0) = A(\epsilon x)\exp(\mathrm{i}x). \end{aligned}\right\} \qquad (3.1)$$

Here, if a_0 is the sound speed and U_c the convection velocity of the phase fronts represented by the $\exp(\mathrm{i}x)$ term, $M_c = U_c/a_0$ is the convection Mach number. There are, for low-speed shear layers, now two small parameters, M_c and ϵ, the latter being the ratio of the wavelength of the hydrodynamic boundary waves to the length of the wave-packet envelope in which those waves are contained.

In place of the solution (2.5) we now have, with the same definition of $\hat{A}$,

$$p(x,y) = \frac{1}{\epsilon}\int_{-\infty}^{+\infty} \hat{A}\left(\frac{k-1}{\epsilon}\right)\exp(\mathrm{i}kx-\gamma y)\,\mathrm{d}k, \qquad (3.2)$$

where

$$\left.\begin{aligned} \gamma &= +(k^2-M_c^2)^{\frac{1}{2}} \quad \text{for} \quad |k| > M_c, \\ \gamma &= -\mathrm{i}(M_c^2-k^2)^{\frac{1}{2}} \quad \text{for} \quad |k| < M_c. \end{aligned}\right\} \qquad (3.3)$$

For $x^2+y^2 \rightarrow \infty$, use of the method of stationary phase gives

$$p(r,\theta) \sim \frac{1}{\epsilon}\left(\frac{2\pi M_c}{r}\right)^{\frac{1}{2}} \sin\theta \exp(\mathrm{i}M_c r - \tfrac{1}{4}\mathrm{i}\pi)\hat{A}\left(\frac{M_c\cos\theta-1}{\epsilon}\right). \qquad (3.4)$$

In the three particular cases of §2, we have the following:

Case A. Exponential A

$$p \sim \epsilon\left(\frac{2M_c}{\pi r}\right)^{\frac{1}{2}} \exp(\mathrm{i}M_c r-\tfrac{1}{4}\mathrm{i}\pi)\frac{\sin\theta}{[(1-M_c\cos\theta)^2+\epsilon^2]}. \qquad (3.5)$$

Regardless of the ratio ϵ/M_c we can, for $M_c \ll 1$, $\epsilon \ll 1$, develop this in a multipole series, of which the first term is an acoustic dipole, $p \sim \sin\theta$. There is no possibility of a superdirective field for exponential A.

Case B. Algebraic A

$$p \sim \frac{1}{\epsilon}\mathrm{e}^{-1/\epsilon}\left(\frac{\pi M_c}{2r}\right)^{\frac{1}{2}} \exp\left(\mathrm{i}M_c r - \tfrac{1}{4}\mathrm{i}\pi\right)\sin\theta \exp\left(\frac{M_c}{\epsilon}\cos\theta\right). \tag{3.6}$$

Here p is exponentially small in ϵ, rather than algebraically as in (3.5), but the field (3.6) will have a superdirective character provided $M_c/\epsilon = O(1)$ as $M_c \to 0$, $\epsilon \to 0$. This simply means that the envelope width ϵ^{-1} and the acoustic wavelength M_c^{-1} should be comparable, and for such an obviously 'non-compact' source one should indeed expect a 'beaming' or strongly directional effect not expressible in multipole terms (Lighthill 1978, §1.12).

Case C. Gaussian A

$$p \sim \frac{1}{\epsilon}\left(\frac{2\pi M_c}{r}\right)^{\frac{1}{2}} \exp\left(\mathrm{i}M_c r - \tfrac{1}{4}\mathrm{i}\pi\right)\sin\theta\left(\frac{1}{2\pi^{\frac{1}{2}}}\right)\exp\left\{-\frac{1}{4\epsilon^2}(1-M_c\cos\theta)^2\right\}$$

$$\sim \frac{1}{\epsilon}\mathrm{e}^{-1/4\epsilon^2}\left(\frac{M_c}{2r}\right)^{\frac{1}{2}} \exp\left(\mathrm{i}M_c r - \tfrac{1}{4}\mathrm{i}\pi\right)\sin\theta\exp\left(\frac{M_c}{2\epsilon^2}\cos\theta\right). \tag{3.7}$$

Here p is even smaller (with respect to ϵ) than in Case B, $p \sim \epsilon^{-1}\exp(-1/4\epsilon^2)$, but again there is the possibility of a superdirective field. This requires

$$M_c/\epsilon^2 = O(1) \tag{3.8}$$

and allows the acoustic wavelength M_c^{-1} to be large, $O(\epsilon^{-2})$, compared with the envelope scale ϵ^{-1}. The wave packet appears to be *compact*, in that as $M_c \to 0$ its physical envelope scale along the boundary $y = 0$ is a vanishingly small fraction of the acoustic wavelength – and yet it has a superdirective non-multipole field at infinity.

It is possible to analyse the Gaussian for compressible flow more fully. If we write $(\bar{x}, \bar{y}) = (M_c x,\ M_c y)$ for the Helmholtz coordinates appropriate to the wave field, then for the Gaussian, equation (3.2) reads

$$p = \frac{\epsilon}{2\pi^{\frac{1}{2}}}\mathrm{e}^{-1/4\epsilon^2}\int_{-\infty}^{+\infty}\exp\left\{-\tfrac{1}{4}\epsilon^2u^2 + \mathrm{i}u\bar{x} + \tfrac{1}{2}u - \bar{y}(u^2-1)^{\frac{1}{2}}\right\}\mathrm{d}u, \tag{3.9}$$

where we have taken $M_c = \epsilon^2$ for definiteness, in view of (3.8). If $\bar{y} > \frac{1}{2}$ ($\tilde{Y} > 0$ in the notation of (2.16)), we can drop the first term in the exponential, leaving the integral as

$$F(\bar{x}, \bar{y}) = \int_{-\infty}^{+\infty}\exp\left(\mathrm{i}u\bar{x} - \bar{y}(u^2-1)^{\frac{1}{2}} + \tfrac{1}{2}u\right)\mathrm{d}u.$$

The contributions to F from $|u| > 1$ (the non-radiating wavenumber range) represent a field of essentially hydrodynamic type which is $O(\bar{y}^{-2})$ as $\bar{y} \to +\infty$. The contribution from $|u| < 1$ gives the acoustic field

$$F_a(\bar{x}, \bar{y}) = \int_{-1}^{+1}\exp\left(\mathrm{i}u\bar{x} + \mathrm{i}\bar{y}(1-u^2)^{\frac{1}{2}} + \tfrac{1}{2}u\right)\mathrm{d}u, \tag{3.10}$$

in which the far-field approximation has not yet been made. This shows that when $r = O(\epsilon^{-2})$ there is a clear interaction in (3.10) between the acoustic oscillations represented by the term $\exp[\mathrm{i}u\bar{x} + \mathrm{i}\bar{y}(1-u^2)^{\frac{1}{2}}]$ and the phase variation imposed at the boundary and still present in (3.10) through the term $\exp(\frac{1}{2}u)$. In the very distant field, $r \gg \epsilon^{-2}$, stationary phase yields (3.7) again, $\exp(\frac{1}{2}u)$ giving the superdirective term.

The condition (3.8), or its analogue for other A, is simply the requirement that the *penetration distance be comparable with the acoustic wavelength*. This can be understood from a matching approach. We seek to solve (3.1) by matched expansions, as $M_c \to 0$, for various fixed relations between M_c and ϵ. We need a set of coordinates to describe the incompressible motions, and another for the compressible solutions to the Helmholtz equation. Imagine M_c^{-1} to be much larger than any length scale associated with the incompressible fields of §2, $M_c^{-1} \gg \delta$, where $\delta = \epsilon^{-1}\Delta$ is the penetration distance in the (x, y) variables. Then for the acoustic field we have to solve

$$\frac{\partial^2 \bar{p}}{\partial \bar{x}^2}+\frac{\partial^2 \bar{p}}{\partial \bar{y}^2}+\bar{p} = 0, \tag{3.11}$$

with $(\bar{x}, \bar{y}) = (M_c x, M_c y)$ the Helmholtz coordinates, and as $(\bar{x}, \bar{y}) \to 0$, $\bar{p}$ must match the algebraically decaying incompressible dipole field in which $p \sim \sin\theta/r$. This can only be achieved if $\bar{p}$ is itself a compressible dipole solution, $\bar{p} \sim H_1^{(1)}(\bar{r})\sin\theta$, of (3.11).

Such an argument for the acoustic dipole nature of $\bar{p}$ will *fail* when M_c^{-1} becomes comparable with the penetration distance δ. For exponential $A(X)$ this is never possible, for then $\delta = 1 \ll M_c^{-1}$, and the field is therefore always dipole – in agreement with the conclusion drawn from (3.5). For algebraic $A(X)$ it is possible, and there will be non-multipole behaviour if $M_c^{-1} \lesssim \epsilon^{-1}$, while $M_c^{-1} \lesssim \epsilon^{-2}$ is required for Gaussian $A(X)$ – again as already deduced. The result for algebraic $A(X)$ is as expected – the wave-packet envelope must be non-compact in the usual sense; that for Gaussian is unexpected in that the wave-packet envelope remains highly compact.

For the higher-order Gaussian behaviour, suppose that $\hat{A} \sim \exp(-|K|^{2n})$, as $|K| \to \infty$. Then the acoustic field is of the form

$$p \sim \exp\left(-\frac{1}{\epsilon^{2n}}\right)\left(\frac{1}{r}\right)^{\frac{1}{2}} \exp(\mathrm{i}M_c r)\sin\theta \exp\left(2n\frac{M_c}{\epsilon^{2n}}\cos\theta\right), \tag{3.12}$$

and is superdirective if $M_c \sim \epsilon^{2n}$ which, in view of (2.23), is again the condition for comparability of δ and M_c^{-1}.

These ideas are not, however, in conflict with standard acoustic theory if the source scale is correctly defined – which here requires accurate allowance for phase cancellation effects rather than reference to the wave-packet scale alone. (We are indebted to a referee for pointing this out, and thereby removing a misconception on our part.) What matters for acoustic purposes is the integral scale $l(\epsilon)$, defined such that

$$\int_{-l}^{+l} A(\epsilon x)\,\mathrm{e}^{\mathrm{i}x}\,\mathrm{d}x \sim \int_{-\infty}^{+\infty} A(\epsilon x)\,\mathrm{e}^{\mathrm{i}x}\,\mathrm{d}x,$$

as $\epsilon \to 0$, or more conveniently, such that

$$\int_{-\infty}^{+\infty} B\left(\frac{x}{l}\right) A(\epsilon x)\,\mathrm{e}^{\mathrm{i}x}\,\mathrm{d}x \sim \int_{-\infty}^{+\infty} A(\epsilon x)\,\mathrm{e}^{\mathrm{i}x}\,\mathrm{d}x, \tag{3.13}$$

for some smooth $B(\mathscr{L})$ with $\int_{-\infty}^{+\infty} B(\mathscr{L})\,\mathrm{d}\mathscr{L} = 1$ and $B(\mathscr{L})$ vanishing rapidly for $|\mathscr{L}| \gg 1$. But the left-hand side of (3.13) is

$$\frac{1}{\epsilon^2 l}\left\{\hat{A}\left(-\frac{1}{\epsilon}\right)B(0)+\frac{1}{\epsilon l}\frac{\partial \hat{A}}{\partial K}\left(-\frac{1}{\epsilon}\right)B'(0)+\dots\right\}, \tag{3.14}$$

so that (3.13) will be satisfied by

$$\epsilon l \sim \frac{\partial}{\partial K}[\ln \hat{A}(K)]_{K=-\frac{1}{\epsilon}}, \tag{3.15}$$

in agreement with the definition (2.22) of the penetration distance.

As presented here, these arguments simply give the conditions under which non-multipole behaviour is to be expected or not, depending on the ratio of acoustic wavelength to the penetration distance or integral scale. They do not indicate what sort of far field is to be expected when it is non-multipole, but one may generally expect a superdirective field involving exponentials of cosines. The reason is that, when the acoustic wavelength exceeds δ, the field at the beginning of the acoustic region has lost all information about the wave-phase structure which was present at the boundary, and remembers the boundary data only through the total force F_0 which figures in (1.6). Consequently, the acoustic field can have no better recall of the boundary data, and must have a multipole character. If, on the other hand, δ and M_c^{-1} are comparable, the acoustic field will be driven (as in (3.10), for example) by an inner incompressible field which still retains some boundary-phase structure, and the far field will have an exponential 'antenna factor' reflecting that structure.

4. The Laufer–Yen experiment

The envelope fitted by Laufer & Yen (1983) to their experimental data (for the fundamental and first two subharmonics) is quoted in (1.1), and if the unit of length is chosen to make $p \sim \exp \mathrm{i}x$ for the fast oscillations, it follows that, in our notation, $\epsilon = (2\pi)^{-1}$ and $A(\epsilon x) = \exp(-\epsilon^2 x^2)$. At a jet Mach number of 0.1 the convection Mach number is 0.05, and clearly, then, the conditions for a superdirective field are met; indeed $(M_c/2\epsilon^2)$ in (3.7) is very close to unity. According to (3.7), $\langle p^2 \rangle$ would be expected to vary as $\exp(40M_c \cos\theta)$, which is of the right form to explain one of the most puzzling features of the experiment, though not with sufficient variation to agree with the extraordinarily rapid variation $\exp(90M_c \cos\theta)$ quoted in (1.2).

There are, of course, many other factors contributing to the measured directivity (1.2) which are not correctly modelled here, and it is inappropriate to pursue the comparison further until a more detailed analysis of the shear-layer dynamics is available to predict $A(\epsilon x)$. This will be reported in a forthcoming paper. In the meantime, the present paper has shown, through simple model problems which have much in common with the essential features of the Laufer–Yen experiment, how a wave-packet source of particular structure can be highly compact in a nominal sense, and yet have a superdirective acoustic field.

5. Conclusions

We have examined the near-field pressure decay and the acoustic far-field directivity generated by boundary data of wave-packet form $A(\epsilon x)\exp(\mathrm{i}x-\mathrm{i}t)$. Exponential decay of incompressible pressure fluctuations is found to change to algebraic at a penetration distance $O(1)$, $O(\epsilon^{-1})$ and $O(\epsilon^{-2})$ for three representative envelope functions, $A(X) = \exp(-|X|)$, $A(X) = (1+X^2)^{-1}$ and $A(X) = \exp(-X^2)$, respectively. For the acoustic field, matching arguments indicate that superdirective behaviour will be found when the penetration distance and wavelength are comparable, a condition that can be met for a Gaussian $A(X)$ with an envelope scale which is a vanishing fraction, $O(\epsilon)$, of the acoustic wavelength. This appears to contradict the standard requirement for superdirectivity, that the 'source scale' must be comparable with the acoustic wavelength. However, the apparent contradiction is resolved by the recognition that the integral scale of the source, the proper measure of its size for acoustic purposes, is $O(\epsilon^{-2})$ for Gaussian A (and indeed the integral scale and penetration distance are comparable for any A).

The general relationship between these near- and far-field features and those found in low-Mach-number jet flows has been explained. In particular, the predicted hyperbolic near-field pressure contours of a Gaussian envelope fit the contours measured by Lafouasse *et al.* (1986), while the Gaussian envelope of large-scale waves on a round jet was predicted by Huerre & Crighton (1983) and measured by Laufer & Yen (1983) along with the associated superdirective radiation – all in the surprising case of a very-low-Mach-number jet ($M_J = 0.1$), with wave packets of large width $\epsilon^{-1} \sim 2\pi$.

We are grateful to one of the referees for particularly helpful comments, as noted in §3, and to Dr J. M. Rallison for helpful comments in relation to the criterion (2.22). This work was supported by AFOSR Grant number AF F 49620-82-K-0019, and was reported in preliminary form as paper *AIAA*-84-2295 at the AIAA/NASA 9th Aeroacoustics Conference, Williamsburg, October 1984.

REFERENCES

CRIGHTON, D. G. & HUERRE, P. 1984 *AIAA*-84-2295.

GUTMARK, E. & HO, C.-M. 1985 *AIAA J.* **23**, 354–358.

HUERRE, P. & CRIGHTON, D. G. 1983 *AIAA*-83-0661.

LAFOUASSE, B., CHAN, A. & HO, C.-M. 1986 *Proc. IUTAM Symp. on Aero- and Hydro-Acoustics, Lyon 1985* (ed. G. Comte-Bellot & J. E. Ffowcs Williams), pp. 403–409. Springer.

LAUFER, J. & YEN, T. C. 1983 *J. Fluid Mech.* **134**, 1–32.

LIGHTHILL, J. 1978 *Waves in Fluids*. Cambridge University Press.

LIGHTHILL, M. J. 1952 *Proc. R. Soc. Lond.* A **211**, 564–587.